

W-Ni-Fe nanostructure materials synthesized by high energy ball milling^①

FAN Jing-lian(范景莲), HUANG Bai-yun(黄伯云), QU Xuan-hui(曲选辉)
State Key Laboratory for Powder Metallurgy, Central South University of Technology,
Changsha 410083, P. R. China

Abstract: Investigations were made on the phase evolution and thermal stability of the 90W-7Ni-3Fe (mass fraction, %) milled powders by means of XRD and DTA. The results showed that ball milling produced an ultrafine composite powder consisting of supersolidus solution W(Ni, Fe) and amorphous phase, owing to the fast diffusion rate induced by high density of lattice defects and nanograin boundaries. The amorphous phase results from the extension of the solubility of W in γ (Ni, Fe) phase which forms during the first 3 h of ball milling.

Key words: heavy metal alloy; mechanical alloying; nanostructure

Document code: A

1 INTRODUCTION

Tungsten based alloys are unique materials due to the combination of high density, strength, ductility, conductivity, machinability and formability. Fully densified tungsten heavy alloy is prepared typically via liquid phase sintering of W powder blended with Ni and Fe powders. However, the high sintering temperature and long sintering time result in coarse microstructure and progressive compact slumping and distortion^[1-5]. Ultrafine metal powders have been reported as one of the advanced materials because of their large specific surface area and high reactivity^[6]. The most attractive method to produce nanograin powders is high energy ball milling. It is also gradually attractive in tungsten heavy alloy to refine microstructure and enhance consolidation to reduce sintering temperature^[7-10]. But fewer studies on characteristics of the as-milled powders from microstructural change and thermal analysis have been reported. In this paper, based on XRD and DTA, we would like to study the as-milled powder characterization during milling in detail.

2 EXPERIMENTAL

The initial W(99.95%, 2.91 μm), Ni(99.5%, 2.66 μm) and Fe(97.0%, 6.50 μm) powders were mixed in a mass proportions of 90:7:3, then subjected to mechanical alloying.

Milling was conducted in a QM-1 planetary ball mill equipped with 100 mL stainless vials. Stainless balls, cemented carbide balls or tungsten balls were used. The mass ratio of balls to powder was 5:1. The rotation rate was 200 r/min. The experiments were carried out in a high purity argon atmosphere.

After various times of milling, a small amount of

mechanically alloyed powders were extracted from the container and glued onto a silica plate for XRD tests. The XRD patterns were obtained with $\text{CuK}\alpha$ radiation at a scanning rate of 0.1 ($^\circ$)/s. Using a combination of W (110) with W (321) peaks, the grain size and lattice distortion were calculated according to the following equation^[11]:

$$B \cos \theta = 0.94 \lambda / D + 2 \varepsilon \sin \theta \quad (1)$$

where B was peak integral width, θ Bragg angle, D grain size, ε lattice distortion, and λ X-ray wave length.

The relative integral intensity ratio of W to Ni, R , was determined in terms of

$$R = I_{\text{W}(110)} / I_{\text{Ni}(111)} \quad (2)$$

The DTA thermal analysis was carried out using Perkin Elmer 7 series thermal analysis system. About 30 mg of the as-milled powders were sealed in a copper capsule and were heated from 30 $^\circ\text{C}$ up to 1470 $^\circ\text{C}$ at a fixed heating rate of 10 $^\circ\text{C}/\text{min}$.

3 RESULTS AND DISCUSSION

Fig. 1 shows the variation of X-ray diffraction patterns of the powder mixture milled for different times. Milling causes broadening of the line profiles. The Ni and Fe peaks disappear with increasing milling time and the fcc γ (Ni, Fe) solid solution forms. It has been reported^[11, 12] that the γ phase forms during the first 3 h of milling. With the increase of milling time, the γ (Ni, Fe) Bragg peaks decrease in intensity. The peaks even become invisible for the powder milled for 35 h with tungsten balls as the milling medium. This behavior is further illustrated in Fig. 2, which gives the variation of R as a function of milling time. As shown in this figure, R becomes very large for 30 h milling, thus the γ (Ni, Fe)(111) peak and its intensity become too

small and weak to be detected. This indicates partial amorphization and the formation of W (Ni, Fe) supersolidus solution. During high energy ball milling processes, the powders are collided, extruded, fractured and cold welded repeatedly, resulting in a large amount of grain boundaries. With the increase of the lattice defects and the grain boundaries, the free energy and diffusion rate increase, which may play a dominant role on the formation of the γ supersolidus solution, amorphization and the extension of solubility of W into γ -(Ni, Fe) binder phase. However, using stainless balls as the milling medium, the two peaks still coexist for the powder milled for 40 h, which suggests that the milling media have great effects on the powder phase evolution during milling.

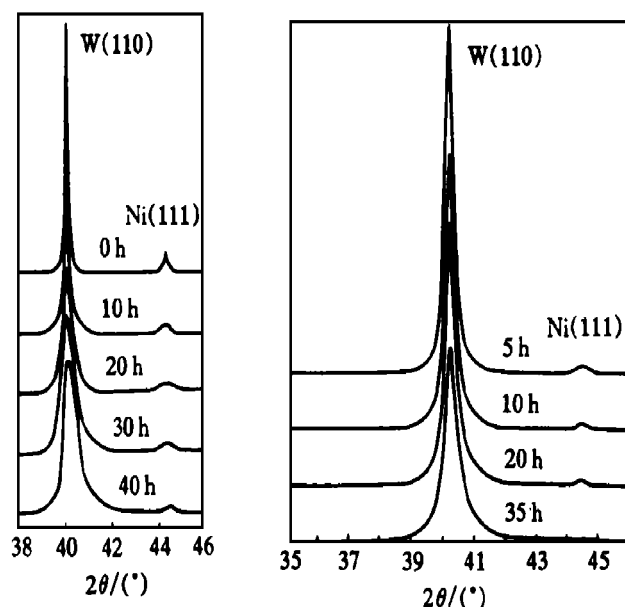


Fig. 1 X-ray diffraction patterns of powder mixture milled for different times
(a) —Using stainless balls; (b) —Using tungsten balls

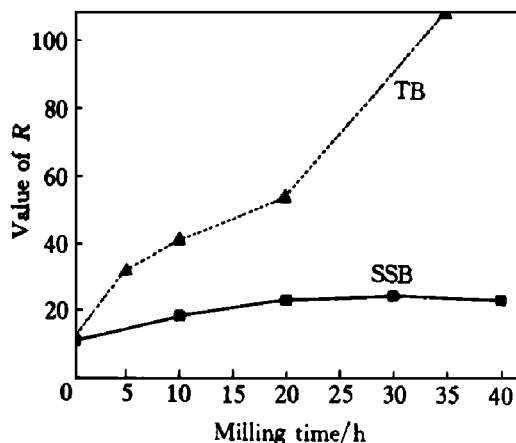


Fig. 2 Relative integral intensity ratio of W(110) to γ phase (111) vs milling time

Therefore, phase evolution can be concluded as follows. At first, due to fast diffusion between Ni and Fe, the γ -solid solution forms and Fe peak disappears. Then, interdiffusion between W, Ni, and Fe leads to increase in solubility of W in γ -(Ni, Fe) and

Ni and Fe in bcc W. When the solubility of W in γ -(Ni, Fe) reaches a certain extent, amorphization occurs^[13]. When the solubilities of Ni and Fe in bcc W surpass those in equilibrium, the supersolidus solution forms.

The broadening of X-ray diffraction line results from the refinement of the crystallite size and intensive lattice distortion. Fig. 3 and Fig. 4 show the relationships between crystallite size D or lattice distortion, $\Delta d/d$ and milling time respectively. It is seen that a rapid decrease in crystallite size and a rapid increase in lattice distortion occur during the first 20 h of milling, due to the balls imparting stronger impact force and energy to powder and powder work hardening. After 30 h of milling, the rate of comminution decreases rapidly, the crystallite size gradually reaches a constant value, and the lattice distortion increases slowly. The impact of the milling media on powder is not high enough to refine the grain size further. The equilibrium between grain recovery and comminution

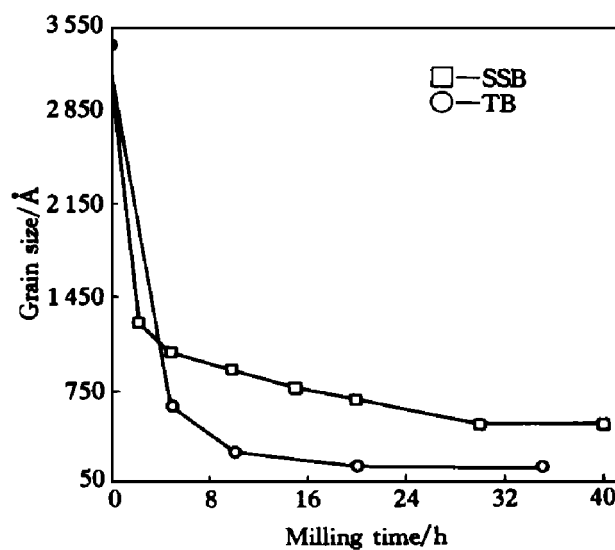


Fig. 3 Variation of crystallite size in tungsten grain as a function of milling time

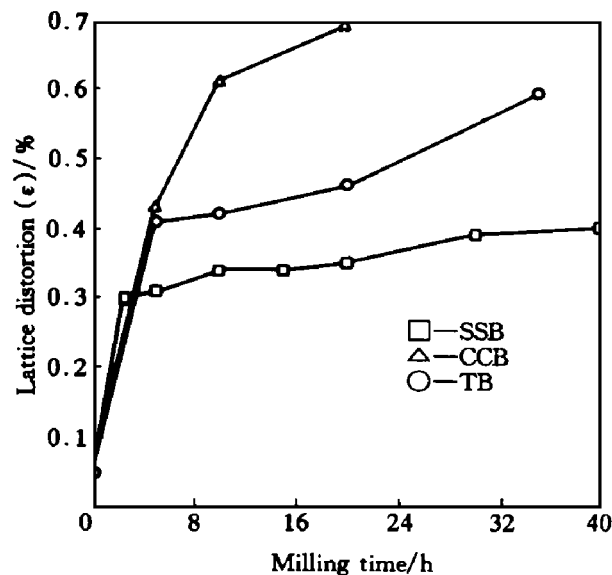


Fig. 4 Variation of lattice distortion in tungsten grain as a function of milling time

is gradually reached. Tungsten or cemented carbide balls has strong impact force, which can refine the crystallite further and aggravate the lattice distortion, thus helping interdiffusion, amorphization and solid solution formation.

The DTA curves show two exothermic and one endothermic peaks with the increase of temperature. The first exothermic peak is relatively broad and flat, ranging from about 200 °C to 750 °C. This is contributed mainly to the exothermal overlapping of precipitation of supersaturated W(Ni, Fe) solid solution, stress relaxation, nano grain recovery and growth. However, the second exothermic peak is narrow and steep, which corresponds to change of amorphous to crystalline formation of W(Ni, Fe) metallic compound and γ (Ni, Fe, W) solid solution. Furthermore, the absolute value of the crystallization enthalpy H (area of the exothermic peak) and the transformation temperature decrease with increasing milling time.

The endothermic peaks in DTA curves correspond to the melting point of γ (Ni, Fe) phase. The melting point is almost not influenced by the increase of milling time, which is different from the report in Ref.[14]. Milling induces a large amount of defects and grain boundaries. The activity of the atoms increases greatly. The free energy and diffusion rate increase, which should decrease the melting point of binder phase. Meanwhile, the interdiffusion rate among W, Ni and Fe increases. According to the Ni-Fe-W phase diagram, the dissolution of W into γ (Ni, Fe) is much easier than that of Ni and Fe into W. Thus, ball milling extends the solubility of W in γ (Ni, Fe) binder phase. The extended solubility certainly increases the melting point. Therefore, the melting point of γ phase remains unchanged with milling time.

4 CONCLUSIONS

1) Nanocrystalline W-Ni-Fe alloyed powders which consist of supersolidus solid solution W(Ni, Fe) and amorphous phase have been obtained by ball milling of Ni, W and Fe elemental powders. The grain size decreases greatly and the lattice distortion increases rapidly with increasing milling time, and stabilizes after 40 h of ball milling.

2) Tungsten balls is a more effective ball milling medium for phase evolution.

3) Phase evolution can be divided into two stages. In the early stage of milling, interdiffusion between Ni and Fe powders leads to the formation of fcc γ (Ni, Fe) solid solution. Then amorphization of fcc γ (Ni, Fe) solid solution occurs and W(Ni, Fe)

supersolidus solution form. The amorphization is due to excessive dissolution of tungsten in fcc γ (Ni, Fe) solid solution.

REFERENCES

- [1] Heaney D F, German R M and Ahn I S. The gravity effect on critical volume fraction liquid phase sintering [A]. In: Alan Lawley and Armour Swanson eds. Advances in powder metallurgy [C]. N J: MPIF, 1993. 169~ 179.
- [2] German R M. Grain agglomeration and coalescence in liquid phase sintering [A]. In: Cadle T M and Narasimhan K S eds. Advances in powder metallurgy [C]. N J: MPIF, 1996. 81~ 97.
- [3] YANG Sung-chul, Mani S S and German R M. Gravitational limit of particle volume fraction in liquid phase sintering [A]. In: Andrett E R and McGeehan P J eds. Advances in powder metallurgy [C]. N J: MPIF, 1990. 469~ 482.
- [4] Mani S S and German R M. Kinetic of gravity induced distortion in liquid phase sintering [A]. In: Andrett E R and McGeehan P J eds. Advances in powder metallurgy [C]. N J: MPIF, 1990. 453~ 467.
- [5] German R M. Limitations in net shaping by liquid phase sintering [A]. In: Pease III L F and Sansoucy R J eds. Advances in powder metallurgy [C]. N J: MPIF, 1991. 183~ 193.
- [6] Sakka Y, Uchikoshi T and Ozawa E. Sintering of copper ultrafine powders [A]. In: Uskokovic D P ed. Science of sintering [C]. N J: Plenum Press, 1989.
- [7] Mukira C G. The Structure and properties of mechanically and consolidated Ni-W(Fe) alloys [A]. In: Bose A and Dowding R J eds. Tungsten refract met-1994, Proc int conf, 2nd [C]. N J: MPIF, 1995. 157~ 167.
- [8] FAN Jing-Lian, QU Xuan-hui, LI Yi-min, *et al.* Sintering of nanocrystalline tungsten heavy alloy powder prepared by high energy ball milling [J]. Journal of Central South University of Technology, (in Chinese), 1998, 29 (5): 450~ 454.
- [9] Gurwell W E. Solid state sintering of tungsten heavy alloy [A]. In: Bose A and Dowding R J eds. Tungsten refract met-1994, Proc int conf, 2nd [C]. N J: MPIF, 1995. 65~ 75.
- [10] FAN Jing-lian, QU Xuan-hui, LI Yi-min, *et al.* Solid state sintering of tungsten heavy alloy [J]. The Chinese Journal of Nonferrous Metals, (in Chinese), 1999, 9 (2): 327~ 329.
- [11] Lonnberg B. Characterization of milled Si₃N₄ [J]. Journal of Materials Science, 1994, 29: 3224~ 3230.
- [12] ZHANG Tong-jun, YANG Jun-you and ZHOU Zhuo-hua. Characteristics of Fe-Ni mechanical alloying during high energy ball milling [J]. Powder Metall Tech, (in Chinese), 1996, 4(1): 3~ 6.
- [13] Aning A O, Whang Z and Courtney T H. Tungsten solution kinetics and amorphization of nickel in mechanically alloyed Ni-W alloys [J]. Acta Metall Mater, 1993, 41(1): 165~ 174.
- [14] Jang J S C and Koch C C. J of Mater Res, 1990, 5(2): 325~ 333.

(Edited by PENG Chao-qun)